NASA TECHNICAL MEMORANDUM

NASA TM X-71914

NASA TM X-71914

INVESTIGATION OF TC-1 FLIGHT FAILURE USING POWER SPECTRAL ANALYSIS

by Carl F. Lorenzo
Lewis Research Center
Cleveland, Ohio 44135

July 1976

1 Report No	2 Government Accession No	3. Recipient's Catalog No
NASA TM X-71914		

4 Title and Subtitle	5 Report Date
INVESTIGATION OF TC-1 FLIGHT FAILURE USING POWER SPECTRAL ANALYSIS	6 Performing Organization Code

7 Author(s)	8 Performing Organization Report No
Carl F. Lorenzo	E-8717
	10. Work Unit No
9. Performing Organization Name and Address	
Lewis Research Center National Aeronautics and Space Administration Cleveland, Ohio 44135	11. Contract or Grant No
	13 Type of Report and Period Covered
12 Sponsoring Agency Name and Address	Technical Memorandum
National Aeronautics and Space Administration Washington, D. C. 20546	14. Sponsoring Agency Code

15 Supplementary Notes

16 Abstract

During the Titan Centaur 1 test flight a failure involving at least one of the Centaur propellant boost pumps occurred. Also, neither of the boost pump speed instruments indicated pump rotation. Accelerometer data from the Titan Centaur 1 flight failure were analyzed using power spectral density methods to determine boost pump speed during attempted starts of the Centaur. The technique was demonstrated on a reference flight. The hydrogen boost pump speed transient was determined for the TC-1 flight. Other trends are seen in the data. However, these are not believed to be the oxygen boost pump. Discussion of data enhancement techniques is also presented.

17. Key Words (Suggested by Author(s))	18. Distribution Statement
Titan Centaur; Atlas Centaur; Power spectral analysis; Flight failure; Data enhancement; Pump	Unclassified - unlimited

19. Security Classif. (of this report)	20. Security Classif. (of this page)	21. No. of Pages	22 Price*
Unclassified	Unclassified		

* For sale by the National Technical Information Service, Springfield Virginia 22161

INVESTIGATION OF TC-1 FLIGHT FAILURE USING POWER SPECTRAL ANALYSIS

by Carl F. Lorenzo

Lewis Research Center
Cleveland, Ohio 44135

SUMMARY

During the Titan Centaur 1 test flight a failure involving at least one of the Centaur propellant boost pumps occurred. Also, neither of the boost pump speed instruments indicated pump rotation.

Accelerometer data from the Titan Centaur 1 flight failure were analyzed using power spectral density methods to determine boost pump speed during attempted starts of the Centaur. The technique was demonstrated on a reference flight.

The hydrcgen boost pump speed transient was determined for the TC-1 flight. Other trends are seen in the data. However, these are not believed to be the oxygen boost pump. Discussion of data enhancement techniques is also presented.

E-8717

INTRODUCTION

During the Titan Centaur 1 test flight a failure of the Centaur vehicle occurred. Grossly, this failure involved at least one of the Centaur propellant boost pumps. Also, during this flight neither of the boost pump speed measurement instruments gave any indication of boost pump rotation.

In view of the suspected boost pump failure, it was desired to use other telemetered data to determine as far as possible the boost pump speed transients during the attempted starts of the Centaur stage.

It was felt that the use of power spectral density methods would allow maximum use of existing data in terms of determination of boost pump operation. Further, it was felt that the boost pump speed transient information

might be helpful in determining the suspected failure mode of the Centaur boost pump(s).

BASIC SCHEME

The basic philosophy was to apply the power spectral approach to an earlier successful reference flight in which the boost pump speed indicators worked properly. Then the results obtained using power spectral density methods would be compared with those indicated directly by the instruments, thereby validating the power spectral approach. Then, having this tool in hand, to apply it to the TC-1 flight data with greater confidence than would be had by directly applying the techniques. The reference flight selected was the Atlas/Centaur-31 flight.

For purposes of this study, the following quantities are of interest: The autocorrelation function $R_x(\tau)$ is defined by

$$R_x(\tau) = \lim_{T \to \infty} \frac{1}{T} \int_0^T x(t)x(t+\tau)dt$$

The power spectral density function $G_x(f)$ is defined by

$$G_x(f) = 2 \int_{-\infty}^{\infty} R_x(\tau)e^{-j2\pi f\tau}d\tau = 4 \int_0^{\infty} R_x(\tau)\cos 2\pi f\tau \, d\tau$$

This can also be expressed as

$$G_x(f) = \lim_{\Delta f \to 0} \lim_{T \to \infty} \frac{1}{(\Delta f)T} \int_0^T x^2(t, f, \Delta f)dt$$

where $x(t, f, \Delta f)$ is that portion of $x(t)$ in the frequency range of f to $f + \Delta f$ (as obtained by passing $x(t)$ through a sharp cutoff filter of bandwidth Δf at frequency f).

For more details and applications of these functions, see ref. 1 or similar texts. The power spectral density function $G_x(f)$ will have peaks at multiples of one per revolution frequency. The basic data display then will be the so-called 3D or Waterfall plots in which individual plots of power spectral density versus frequency are stacked for successive time slices through the data to give a picture over a desired time period of the frequency content of the signal.

In order to define the pump speed transients with sufficient resolution, the time slice required for each power spectral density plot was necessarily very short. This, therefore, dictates a correspondingly high frequency range for the PSD analysis. The analysis times used in this study were 1 second slices which corresponded to a 500 Hz frequency range, and 1/2 second which corresponded to a 1000 Hz range (display truncated to 750 Hz). The frequency range was considerably above the expected one per revolution of the boost pumps in order to use the harmonic structure to identify the boost pumps against the background noise.

REFERENCE ANALYSIS - ATLAS CENTAUR-31 FLIGHT

A variety of accelerometer locations were edited to determine those most likely to expose boost pump speeds for the Atlas Centaur 31 (AC-31) flight data. Considered first were accelerometer locations common to those of the TC-1 flight at the forward end of the Centaur.

That the distant (forward end) accelerometers were not useful is probably due to the fact that the structural transmission path from the thrust section to the front end of the Centaur would only allow information to be passed from the pumps at a few frequencies associated with the resonances in the structural transfer functions between these two points (namely the transmissibility windows). Several pressures were measured in both the AC-31 flight and the TC-1 flight; however, the frequency bandwidth of the measurement was so low as to preclude their use for this study.

The most likely results for identifying the speed transient on AC-31 were obtained on accelerometers located in the thrust sections of the Centaur stage. Accelerometer locations are shown in fig. 1. The data presented

herein are taken from a single accelerometer CA880 in the thrust section. Unfortunately, there was no accelerometer at this location during the TC-1 flight; however, the data quality of this accelerometer appeared superior to the remaining choices for this application. Therefore, commonality was sacrificed.

The primary results of the power spectral analysis of accelerometer CA880 for the AC-31 flight are shown in figs. 2 and 3. The frequency range is 0 to 500 Hz in all cases and reference times are marked beside the photographs. The photographs also provide some time overlap.

The frequency concentration associated with the boost pumps are readily discerned in the photographs. Also, the harmonic relationship between the frequencies is easily seen.* The constant frequency peaks which are seen in the data are usually structural frequencies (perhaps local) which are constant over sustained periods. The b photographs of the series are marked to show the locus of the PSD peaks. The spectral peaks were read from these plots and tabulated. The lowest frequency mode seen in the figure has been interpretted as the second harmonic of the liquid oxygen boost pump. The next higher frequency (not harmonically related) has been interpretted as the second harmonic of the liquid hydrogen boost pump. The true speed lines as indicated by the speed measuring instrument on the pumps were then determined. The results of these two approaches were then plotted as functions of time (fig. 4 and fig. 5).

It is particularly interesting in this flight that the one per revolution frequency of the hydrogen boost pump at steady state occurred at the same frequency as the two per revolution frequency of the oxygen boost pump. This may indicate some difficulty at separating pumps for the TC-1 flight or in identifying a single pump.

Several observations are made concerning the analysis of data for the AC-31 flight. First of all, in observing the power spectral density plots (figs. 2 and 3) directly, it is noticed that the low frequency end contains a significant amount of noise. This low frequency content is apparently engine

*On viewing these photographs, often the patterns may be more easily recognized by viewing from the end of the paper at small incidence angles.

noise propagated by the structure from the still attached Atlas booster. This noise tends to mask some of the lower frequency power concentrations generated by the boost pumps rotation.

The plots comparing measured speed and PSD implied boost pump speed (figs. 4 and 5) compare very well in shape, but differ somewhat in time. There are several effects which are probably influencing this time mismatch. One of these is accurately starting the power spectral analyzer for the 3D plots which is a manual operation based on a tape time signal This is probably the most important effect. The second effect is a question of sweep rate effect. That is, since the forcing functions (pump speeds) are varying in time and we are sensing an acceleration which is the result of some structural transfer function, we have essentially the sweep rate effect which occurs in a vibration test; namely, the response appears to be delayed in time due to the time necessary for the structural transfer function to reach full value (sinusoidal steady state).

The general results of figs. 4 and 5 appear to be a satisfactory matching when temporal effects are neglected. It was felt that the techniques could be satisfactorily applied to the TC-1 flight data.

TITAN/CENTAUR 1 FLIGHT ANALYSIS

For the Titan/Centaur 1 (TC-1) flight data, a variety of accelerometer locations were edited and studied. The accelerometer CA300 was considered to be the best measurement in terms of boost pump activity standing above the background noise level.

The spectral analysis of the (TC-1) flight is presented in figs. 6 through 14, which covers the period prior to the first attempt to start the engine to the time after second start attempt. Again, the b part of the figures indicates the interpretation of boost pump power spectral concentrations and the associated harmonics. The data of fig. 11 was not used in the speed transient plots but is included here for completeness.

The analysis frequency range of 0 - 1000 Hz was used. This corresponds to a 1/2 second analysis time - the time for each spectral scan in the plots. Only the frequency range of 0 - 750 Hz was displayed in the figures. The

lowest frequency interpretation lines have been interpretted as the second or fourth harmonics of the implied pump speed transients.

The boost pump start signal occurred at 13:55:18.3 for the first start attempt. Stage separation occurs at 13:55:56.7.

It will be noted that the background noise level changes significantly after separation when the Centaur stage does not have the noise inputs contributed by the Titan engine system.

Only a single pump is readily discernible in the plots that are shown. (That is, the curves are in harmonic relationship.) The determination of which pump is being observed in the spectral data can be based on several discriminators. These are 1) Harmonic structure; strength of the various harmonics. 2) The rotor time constants as compared to previous flight; and 3) Use of the hydraulic performance of the pumps in the system (i.e., steady state pressure measurements).

Some attempt was made to use the harmonic structures as a discriminator, but the comparison was difficult and inconclusive.

Based on previous flights of the Centaur, it was known that the time constant of the liquid oxygen boost pump was about 10 seconds, and that of the liquid hydrogen boost pump was 14 seconds. The time constant abstracted from the data for this flight was about 14.5 seconds. In addition, the frequencies associated with the fundamental in this data matched very well with the expected one per revolution frequencies of the hydrogen boost pump. This result, together with the steady state hydraulic data allowed the conclusion that the pump observed in the spectral plots was the hydrogen boost pump. On that basis, the results of these transients interpreted as pump speed has been plotted in figs. 15 and 16 against time in flight for both the first and second start attempts for the Centaur engine system in the TC-1 flight. Also indicated on these plots are various important times in the flight in terms of the engine start sequence.

It will be noted that because of the masking noise of the Titan engines the speed transient cannot be determined at low speeds (frequencies). Also, the steady state speed is a little low compared to the AC-31 flight. That is 7500 rpm compared to 8500 rpm.

LIQUID OXYGEN BOOST PUMP

Several patterns were seen in the spectral plots which were considered to be possible indicators of liquid oxygen boost pump rotation activity. In general, any plots in which at least two harmonic lines were not indicated was rejected as possible lox boost pump indicator.

Two plots which might represent lox boost pump rotation are shown in figs. 17 (fig. 7 repeated) and 18. In both figures the patterns indicated are at the limits of optical perception, and may not be valid. They are presented here only to indicate possible behavior of this lox boost pump.

In fig. 17 the frequency relationship between the two patterns indicated is about 7 to 4. The maximum speed based on the 320 Hz level of the fourth harmonic is 4800 rpm. It is extremely unlikely that this is the lox pump, since the pressure data does not validate such a speed. In fig. 18 the harmonics are in a 2 to 3 relationship; here the maximum frequency is again 320 Hz, which for the third harmonic implies 106 Hz fundamental which relates to a 6360 rpm rotational speed.

It is not likely that either of these patterns is representative of the liquid oxygen boost pump, since the speeds are much higher than would be expected from hydraulic performance. It is believed that these are probably the result of some rotating machinery in the still attached Titan vehicle. Again, the patterns are extremely weak and are at the limits of human perception. It is felt that some technique to enhance these results, to separate out the speed changes from background noise from the Titan engine is desired. How this might be done is explored in the Appendix.

CONCLUDING REMARKS

It has been demonstrated that the use of power spectral methods applied to accelerometer flight data can be used to indicate pump speed by testing the technique against known flight results for the AC-31 flight.

The transient of hydrogen boost pump speed versus time for both attempted engine starts for the TC-1 flight has been established. The results appear to be quite good over most of the range; however, they suffer slightly at low amplitudes due to background noise.

There are patterns in the data of other frequency concentrations which may be other rotating machinery in the vehicle; however, it is not believed that these are representative of the oxygen boost pump. In addition, these patterns are very close to the noise level and are quite difficult to establish as valid.

Some enhancement technique could be applied to these data to remove the effects of Titan engine noise; to either expose the oxygen boost pump speed transient (if it exists) and/or the hydrogen boost pump transient at the low speed condition. Such enhancement procedures have been outlined in the Appendix.

APPENDIX

Some consideration was given to enhancement techniques which could be applied to the TC-1 data. These techniques were not implemented due to hardware problems in transferring the analyzed data from the spectrum analyzer to computers where the enhancement procedure could be performed. However, the techniques which were to have been applied are presented here for their potential value for future problems.

The enhancement problem can be understood by reference to fig. 19. Here it can be seen that the accelerometer being analyzed is receiving information from the two boost pumps along with the undesired information from the Titan stage 11 which is still attached during the early part of the boost pump start transient. The information from the Titan consists of both engine and pump noises as transmitted (colored) by the structural transfer functions.

However, since information is available prior to boost pump start (with only the Titan stage II information arriving at the accelerometer), it should be possible to form a reference spectrum during this period which could then be removed from the data during the boost pump start transient. This process should then yield an enhanced result.

Several techniques to accomplish this are outlined in the paragraphs which follow. In the following material:

G_i is the instantaneous i th (time) unenhanced spectrum

G_{Ei} is the enhanced spectrum at the i th time

and

G_R is a reference spectrum to be defined for each approach

K is a constant

TECHNIQUE 1

For this technique the enhanced spectra is given by the equation:

$$G_{Ei} = \begin{cases} G_i - KG_R \text{ for } G_i - KG_R > 0 \\ 0 \qquad\quad \text{for } G_i - KG_R \leq 0 \end{cases} \tag{A1}$$

where K is greater than zero and will normally be chosen to be less than one. For this case, G_R is a reference spectrum formed prior to boost pump start when only Titan engine noise is being generated. The reference spectrum G_R could be an average of several spectra taken during that period or a single representative spectrum at the choice of the analyst.

The basis of this procedure is to eliminate the effect of the Titan engine noise from the boost pump start transient. Namely, prior to boost pump start an average spectrum called G_R would be generated as

$$G_R = \frac{1}{n} \sum_{i=1}^{n} G_i \tag{A2}$$

It should be noted that this procedure is somewhat artificial in that KG_R can be greater than G_i which would yield $G_{Ei} < 0$ without limiting. With limiting, this can produce flat spots (zero) in the enhanced spectra.

TECHNIQUE 2

For this procedure the enhanced spectra G_{Ei} are formed as

$$G_{Ei} = \frac{G_i}{1 + KG_R} \tag{A3}$$

where G_i and G_R are formed as in technique 1. In this case it is clear that the spectral value of G_{Ei} can never be negative and can never be greater than G_i. This appears to be a much more appropriate manner of eliminating the unwanted noise.

It will be noted that when $G_R = 0$, $G_{Ei} = G_i$ and when G_R is large (for example, because of structural resonance coloring of Titan engine noise), G_{Ei} is reduced in spectral power. This approach does not require the arti-

ficial limiting used in the previous technique.

As a guideline in selecting the value of K, define a reduction ratio R as

$$R = \frac{1 + KG_{R\ MAX}}{1 + KG_{R\ MIN}} \tag{A4}$$

then K is determined to be

$$K = \frac{R - 1}{G_{R\ MAX} - RG_{R\ MIN}} \tag{A5}$$

The reduction ratio R represents the relative reduction of the peak in the reference spectrum relative to the minimum of that spectrum.

It is also noted that the enhancement procedure $G_{Ei} = (G_i/G_R)$ is a special case of Eq. (A3) where K is very large.

TECHNIQUE 3

In this case,

$$G_{Ei} = G_i - KG_R \tag{A6}$$

however, G_{Ri} is now defined as

$$G_{Ri} = \frac{1}{2n}(G_{i-n} + \ldots + G_{i-2} + G_{i-1} + G_{i+1} + \ldots + G_{i+n}) \tag{A7}$$

The objective here is to form a reference spectrum which is representative of the nonchanging part of the 3D display. Removal of this reference spectrum from G_i as indicated in Eq. (A6) should expose those parts of the boost pump speed transient which are changing most rapidly, namely the initial part of the transient. With this approach, when the boost pump speed reaches steady state it would be eliminated from the result. In essence, this technique would expose the non-stationary part of the data.

A variant to this approach would be to weigh the spectra composing G_{Ri} for example

$$G_{Ri} = \frac{1}{2n}(A_{i-n}G_{i-n} + \ldots . A_{i-2}G_{i-2} + A_{i-1}G_{i-1} + A_iG_i + \ldots . A_{i+n}G_{i+n})$$

or

$$G_{ri} = \frac{1}{2\,n \div 1}(A_{i-n}G_{i-n} \ldots . A_{i+h}G_{i+n}) = \frac{1}{2n+1} \sum_{j=i-n}^{i+n} A_jG_j \qquad (A8)$$

TECHNIQUE 4

The above reference spectra (technique 3) can also be applied to technique 2 where

$$G_{Ei} = \frac{G_i}{1 + KG_R} \qquad (A9)$$

Here again only the changing part of the spectra will be exposed, and the possibility of $G_E < 0$ does not exist.

REFERENCE

1. Bendat, Julius S. and Piersol, Allan G.: Measurement and Analysis of Random Data. John Wiley & Sons, 1966.

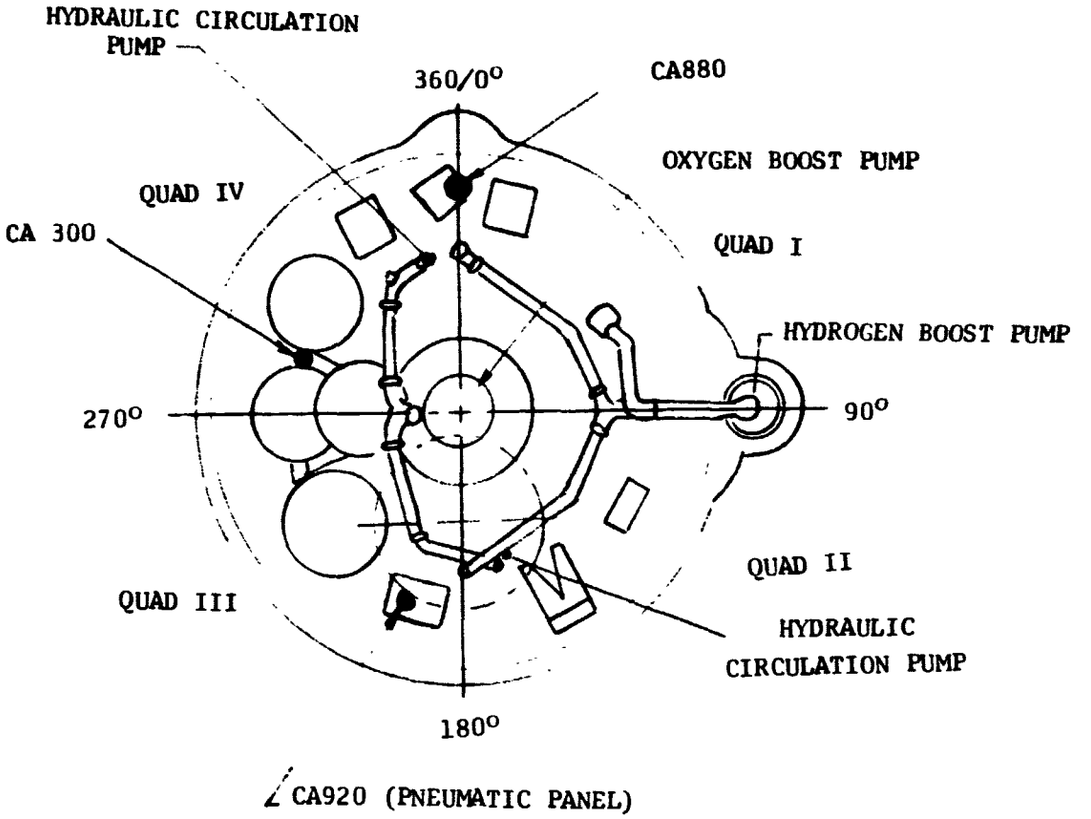

COMMON TC-1 & AC-31

CA930

CA260

CA910

FIGURE 1. ACCELEROMETER LOCATIONS IN CENTAUR THRUST SECTION VIEW LOOKING FORWARD

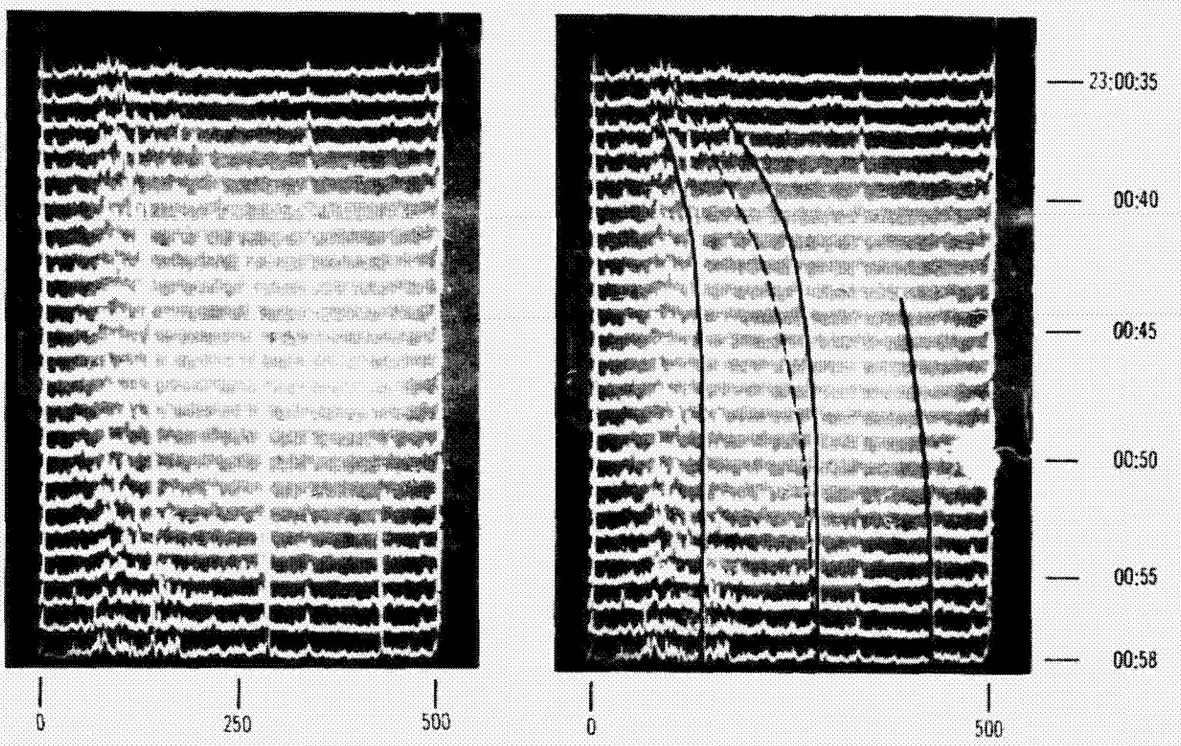

Figure 2. - Acceleration power spectral density versus frequency at 1 second intervals for Atlas Centaur 31 flight. 0 - 500 Hz; accelerometer CA880.

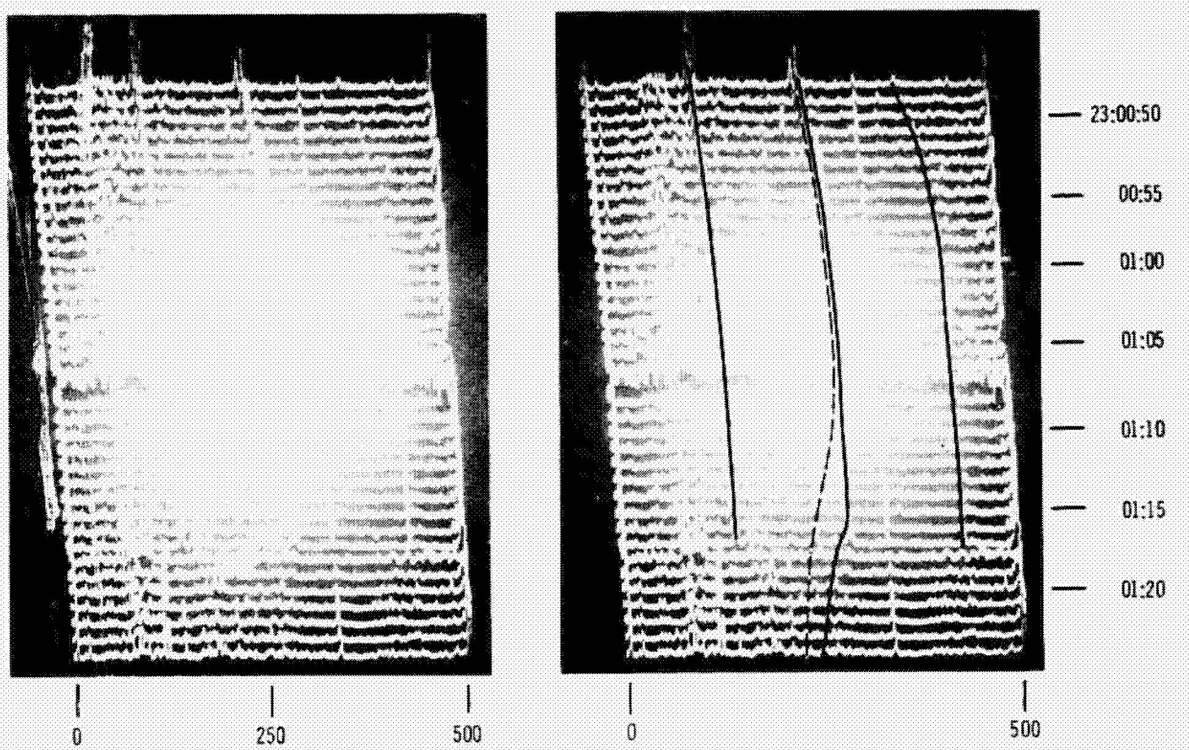

E-6717

Figure 3. - Acceleration power spectral density versus frequency at 1 second intervals for Atlas Centaur 31 flight. 0 - 500 Hz; accelerometer CA880.

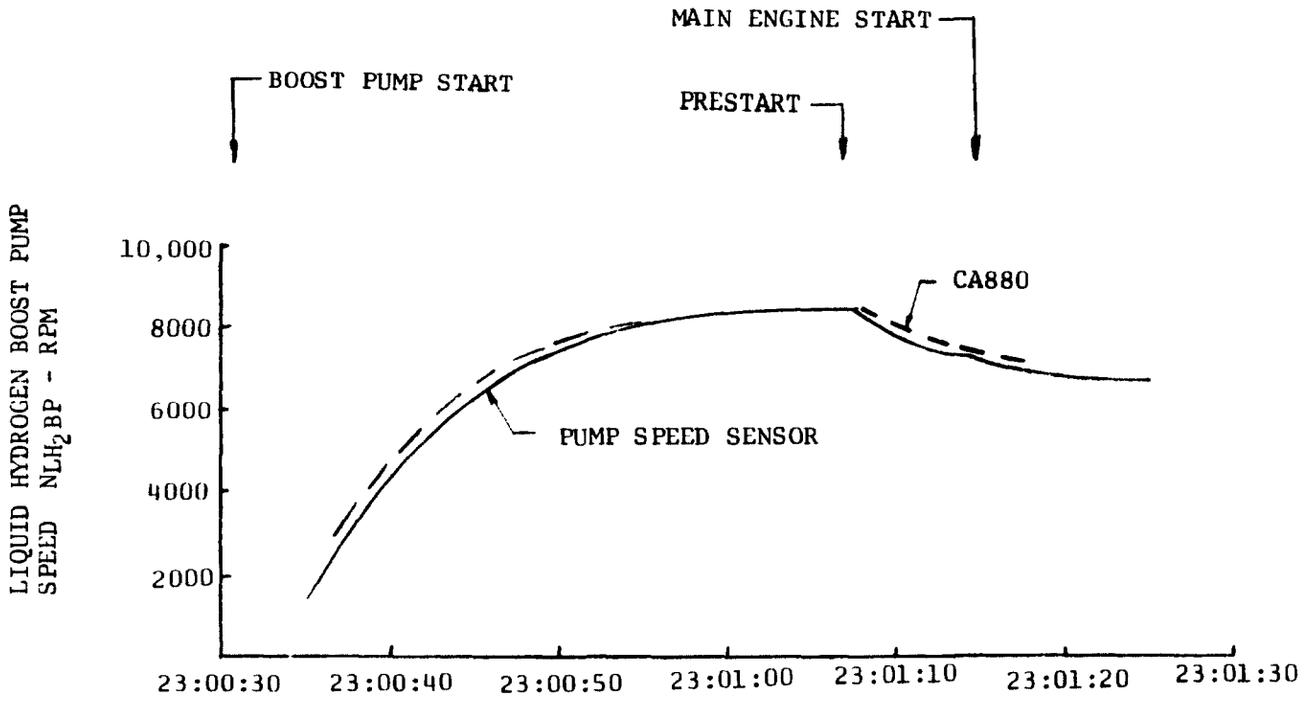

FIGURE 4. COMPARISON OF LIQUID HYDROGEN PUMP SPEED USING SPEED SENSOR AND IMPLIED FROM ACCELEROMETER CA880 FOR AC-31 FLIGHT

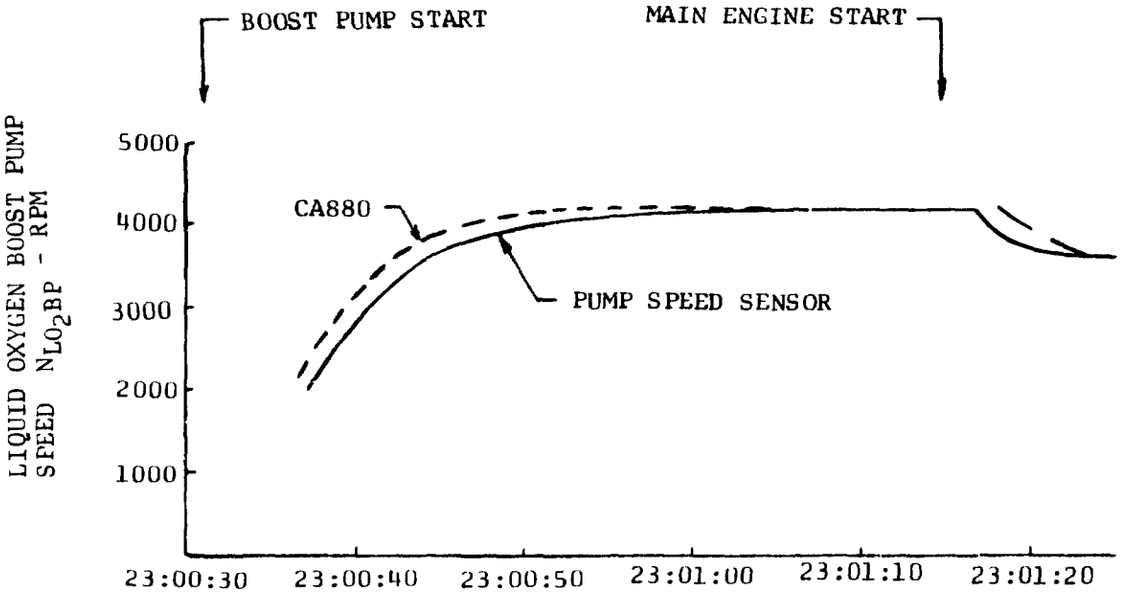

FIGURE 5. COMPARISON OF LIQUID OXYGEN BOOST PUMP SPEED USING SPEED SENSOR AND IMPLIED FROM ACCELEROMETER CA880 FOR AC-31 FLIGHT

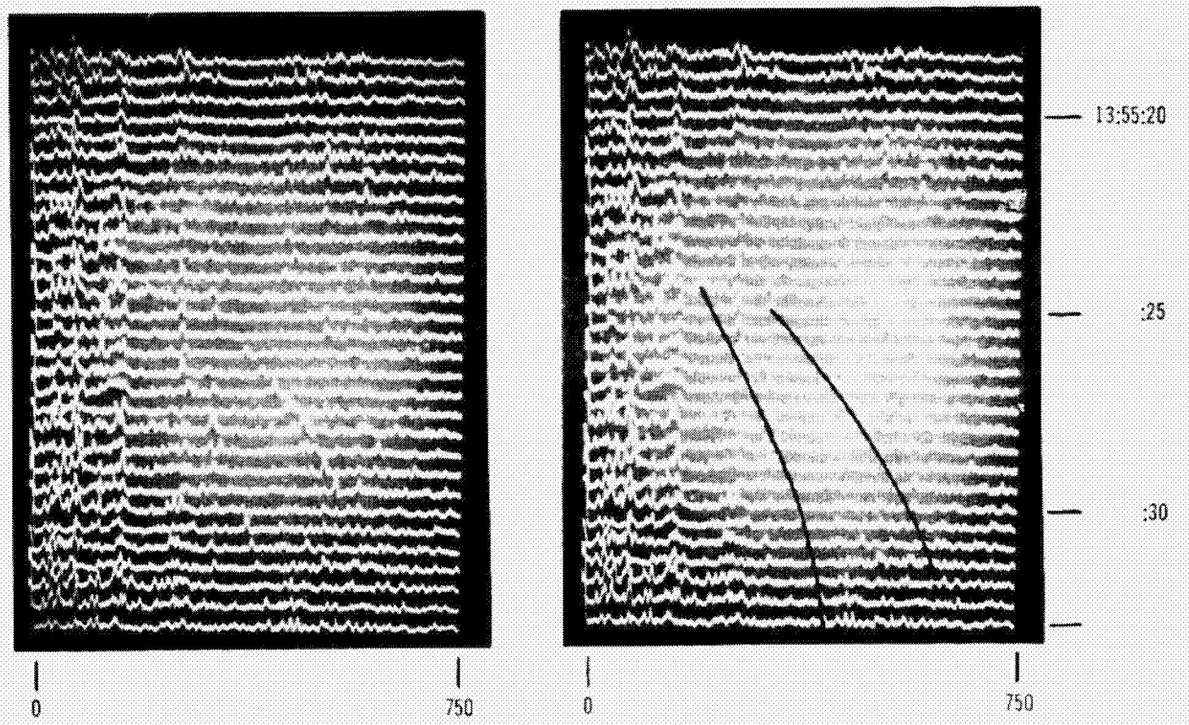

Figure 6. - Acceleration power spectral density versus frequency at $\frac{1}{2}$ second intervals for Titan Centaur 1 flight. 0 - 750 Hz; accelerometer CA300.

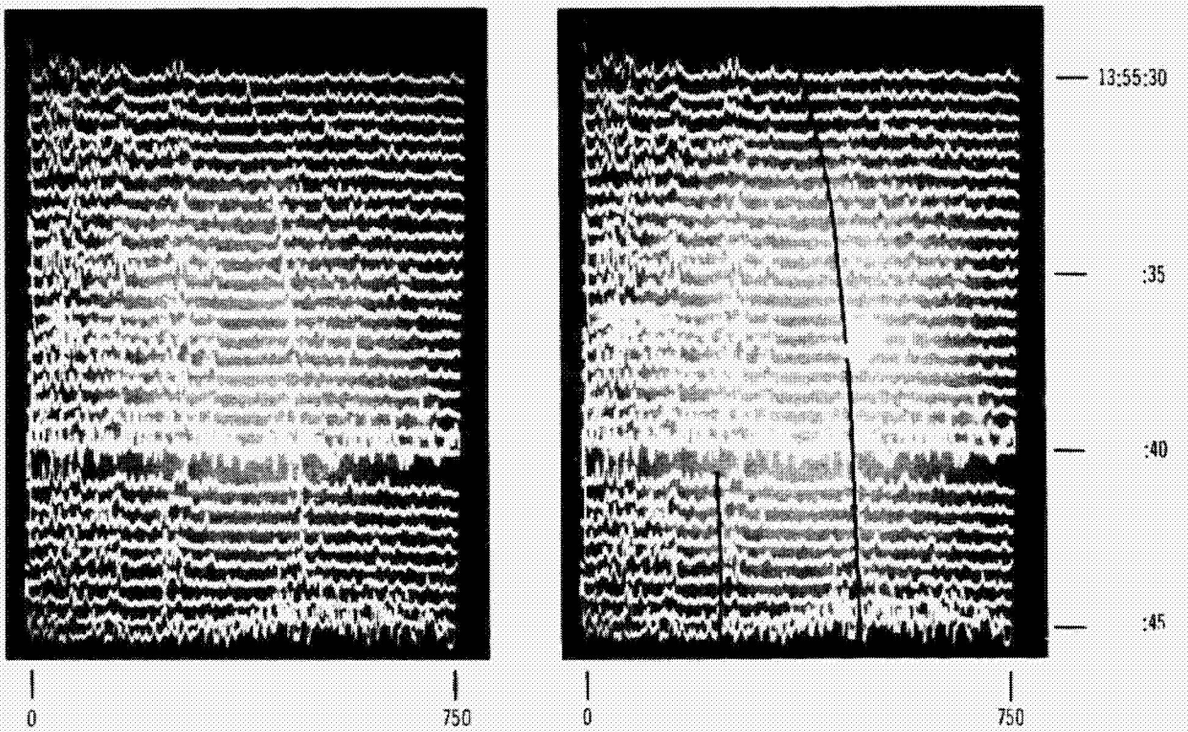

E-6717

Figure 7. - Acceleration power spectral density versus frequency at ½ second intervals for Titan Centaur 1 flight. 0 - 750 Hz; accelerometer CA300.

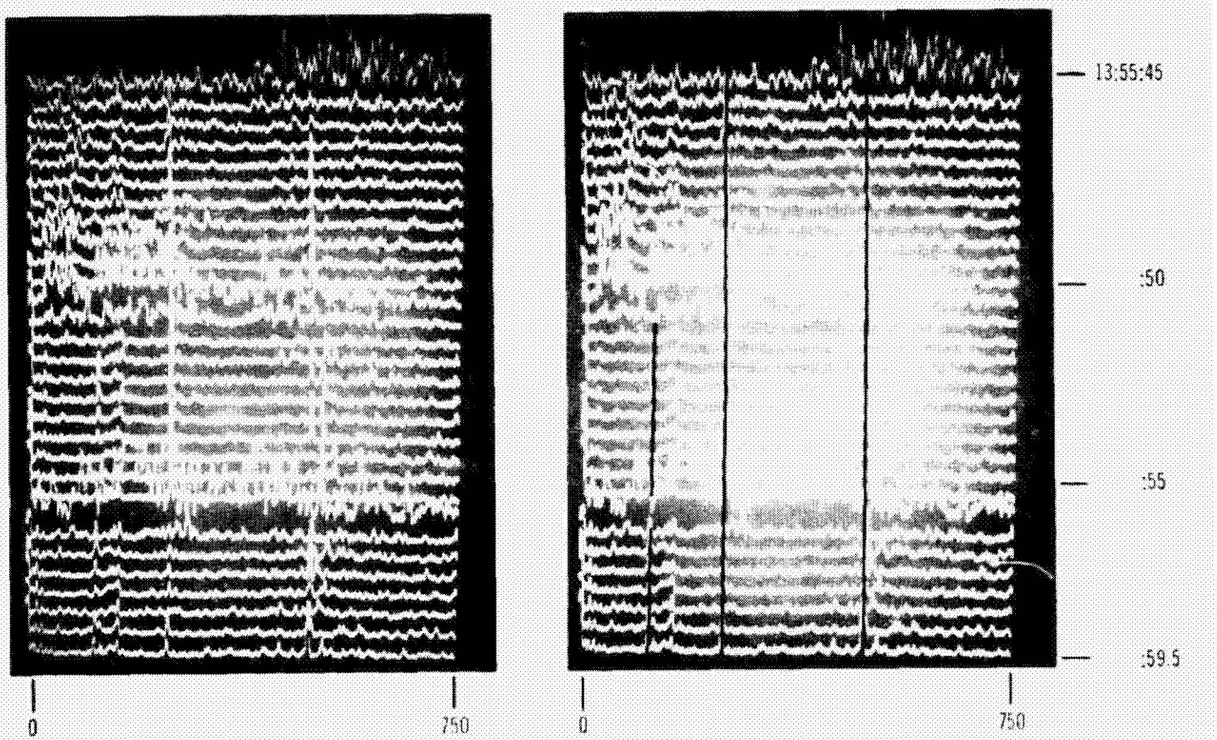

(a) Without interpretation lines

(b) With interpretation lines

Figure 8. - Acceleration power spectral density versus frequency at ½ second intervals for Titan Centaur 1 flight. 0 - 750 Hz; accelerometer CA300.

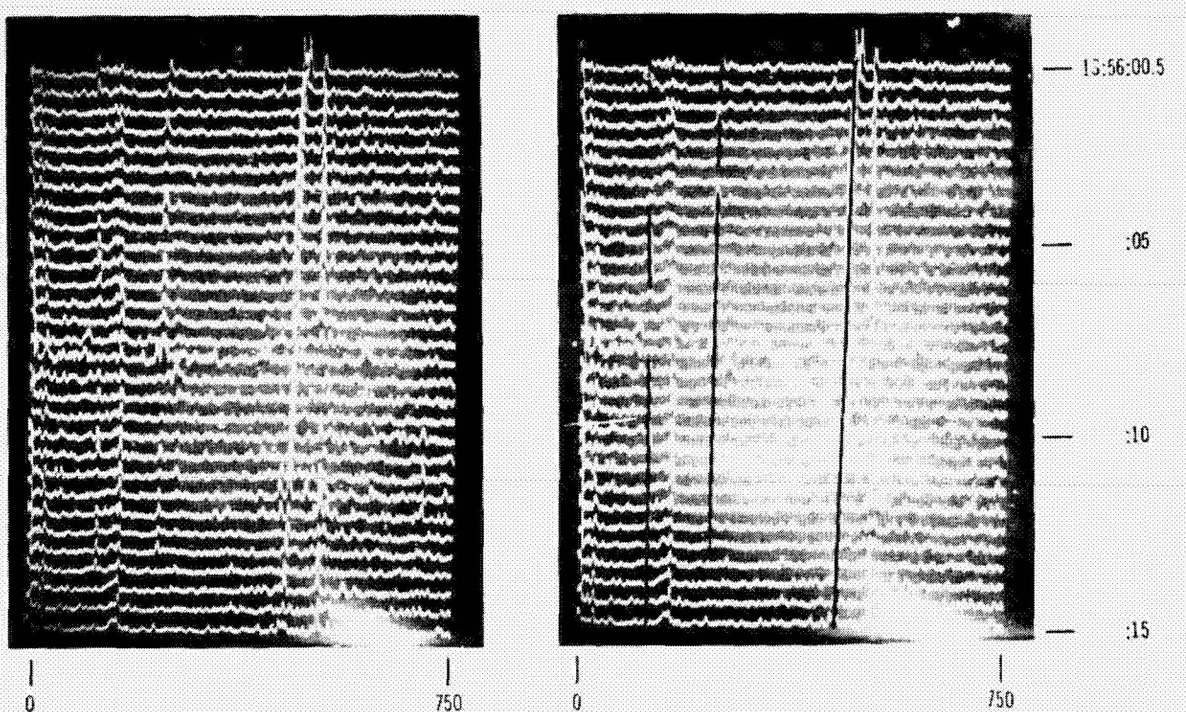

E-8717

Figure 9. - Acceleration power spectral density versus frequency at ½ second intervals for Titan Centaur 1 flight. 0- 750 Hz; accelerometer CA300.

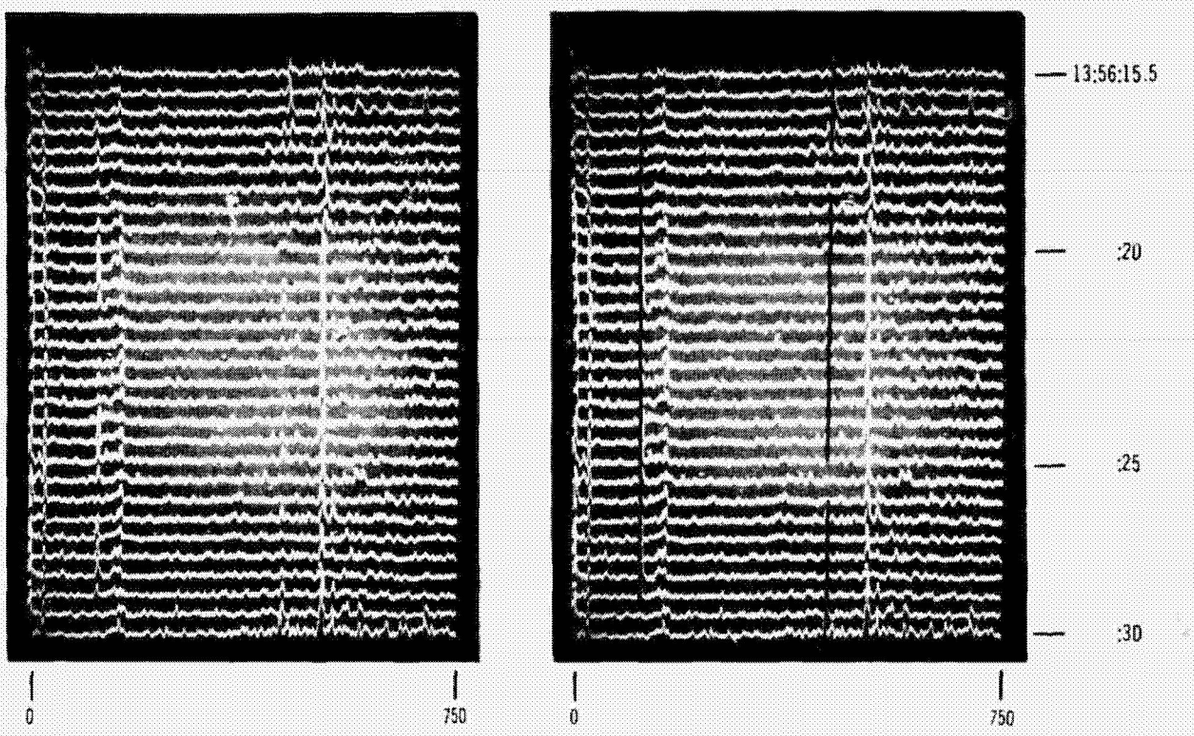

Figure 10. - Acceleration power spectral density versus frequency at ½ second intervals for Titan Centaur 1 flight. 0 - 750 Hz; accelerometer CA300.

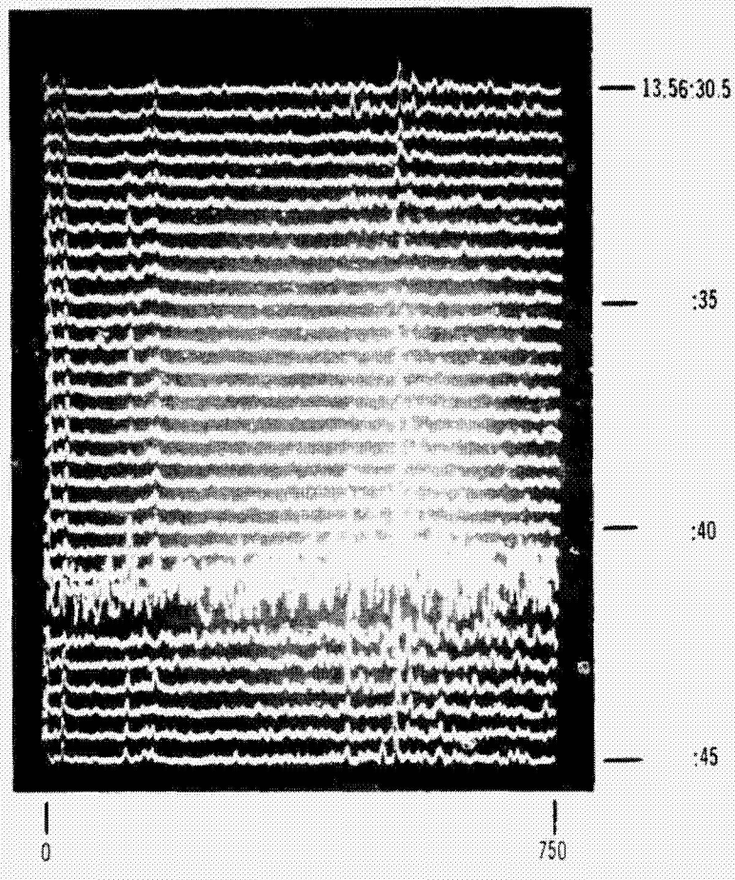

(a) Without interpretation lines

Figure 11. - Acceleration power spectral density versus frequency at ½ second intervals for Titan Centaur 1 flight. 0 - 750 Hz; accelerometer CA300.

E-8717

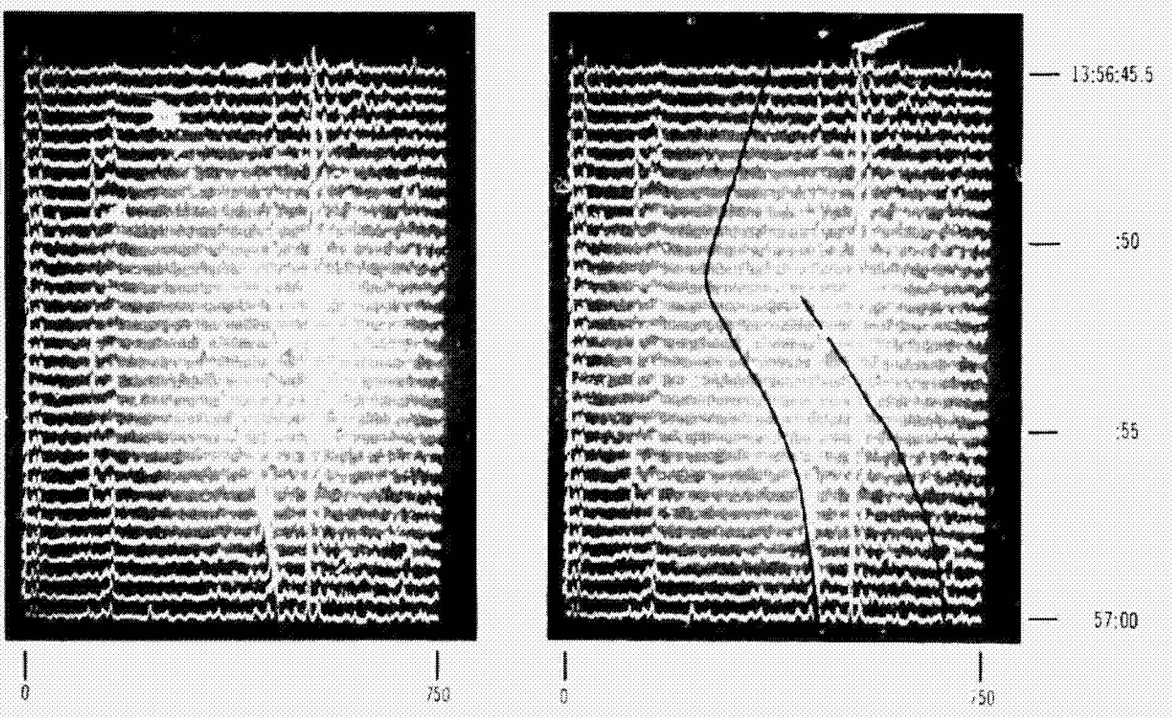

(a) Without interpretation lines

(b) With interpretation lines

Figure 12. - Acceleration power spectral density versus frequency at ½ second intervals for Titan Centaur 1 flight. 0 - 750 Hz; accelerometer CA300.

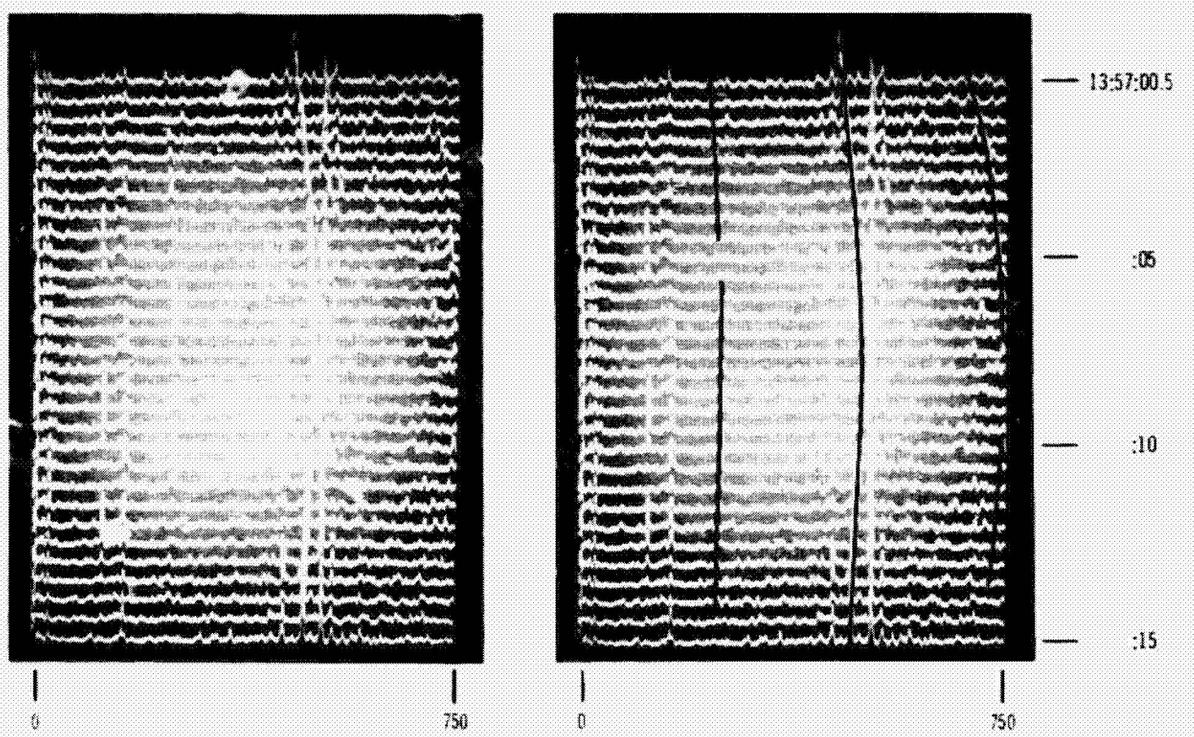

E-6717

(a) Without interpretation lines

(b) With interpretation lines

Figure 13. - Acceleration power spectral density versus frequency at $\frac{1}{2}$ second intervals for Titan Centaur 1 flight. 0 - 750 Hz; accelerometer CA300.

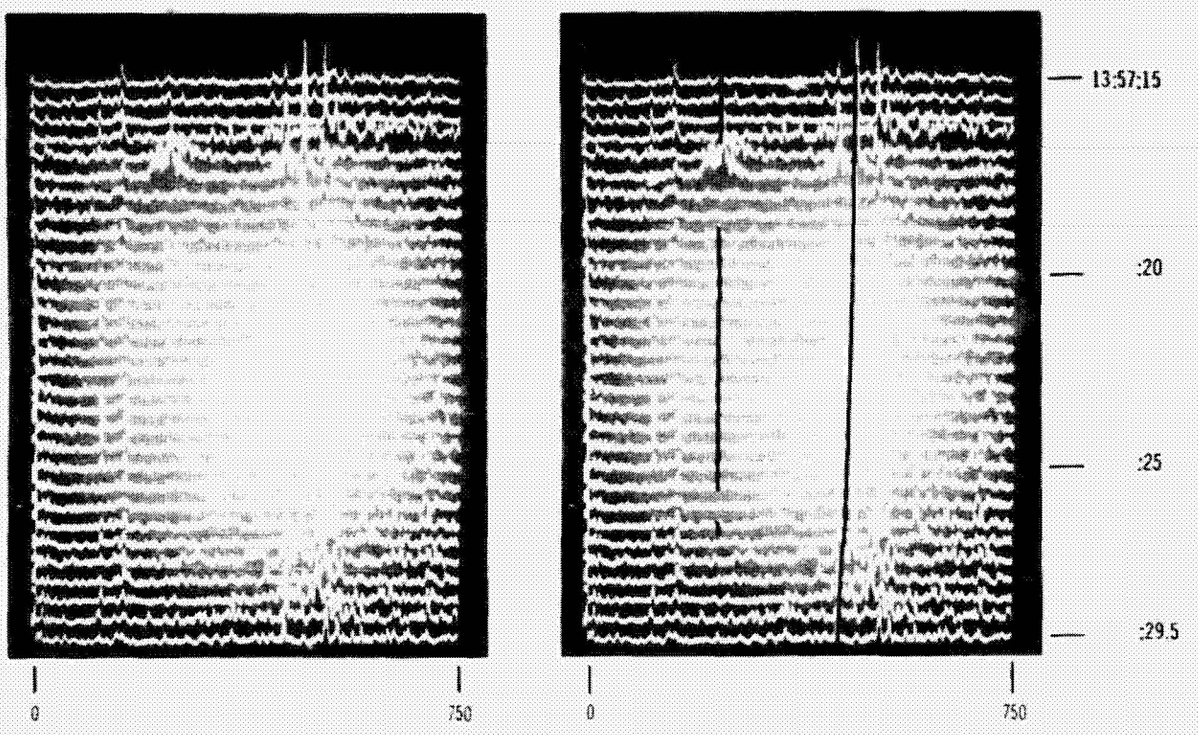

(a) Without interpretation lines

(b) With interpretation lines

Figure 14. - Acceleration power spectral density versus frequency at ½ second intervals for Titan Centaur 1 flight. 0 - 750 Hz; accelerometer CA300.

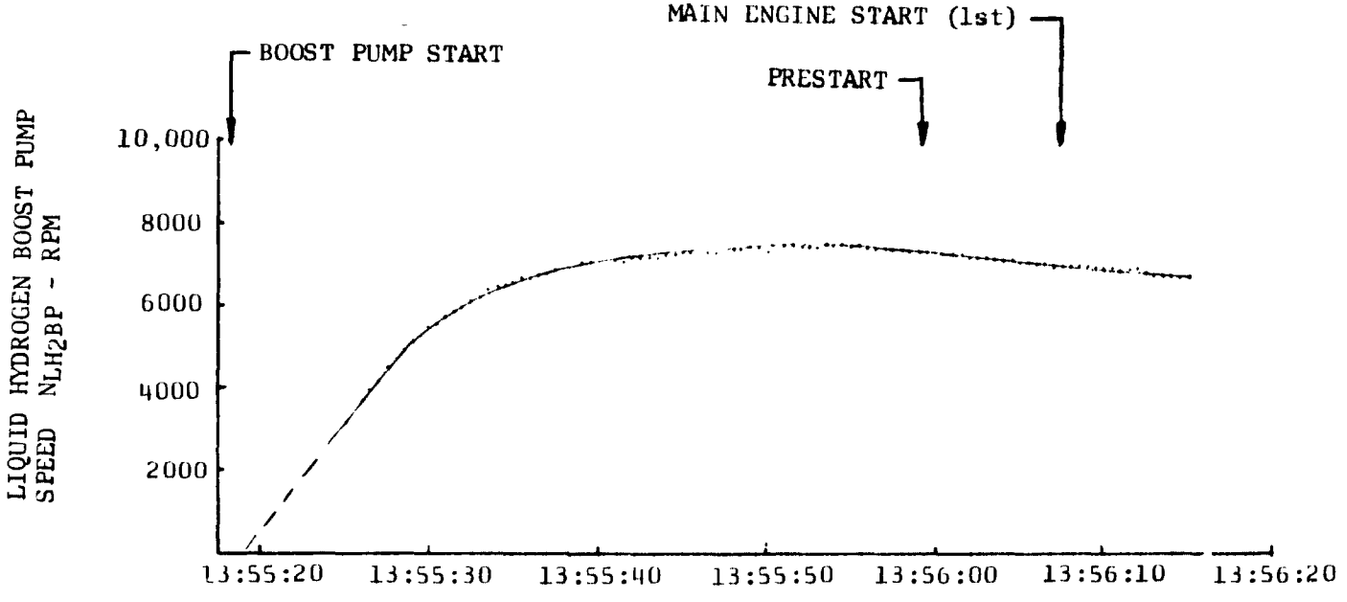

FIGURE 15. LIQUID HYDROGEN BOOST SPEED IMPLIED FROM ACCELEROMETER CA300 FOR TC-1 FLIGHT FIRST START ATTEMPT

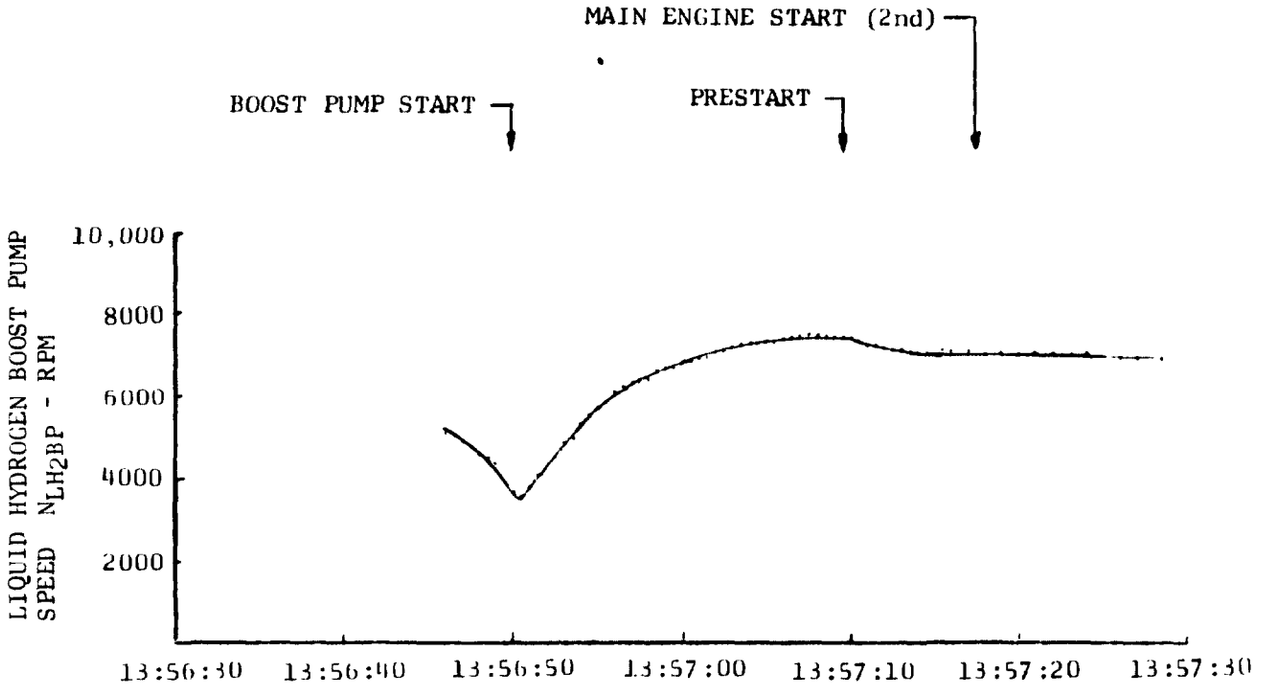

FIGURE 16. LIQUID HYDROGEN BOOST PUMP SPEED IMPLIED FROM ACCELEROMETER CA300 FOR TC-1 FLIGHT SECOND START ATTEMPT

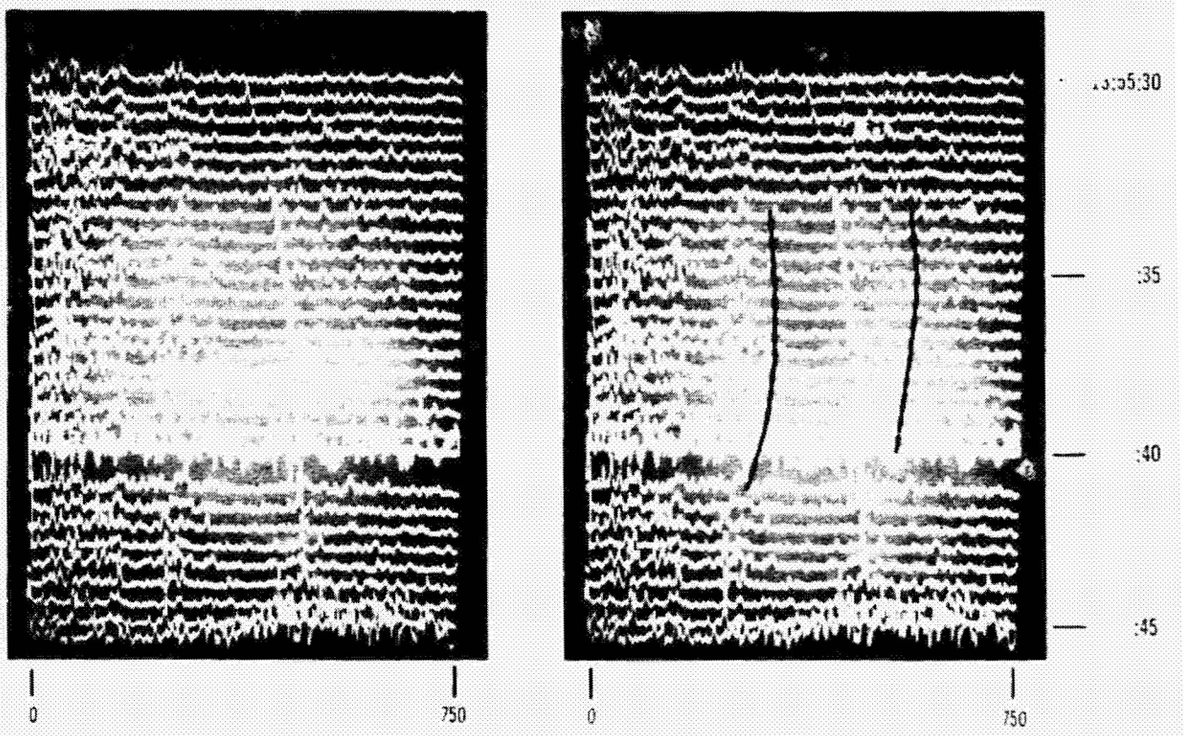

(a) Without interpretation lines

(b) With interpretation lines

E-6717

Figure 17. - Acceleration power spectral density versus frequency at ½ second intervals for Titan Centaur 1 flight. 0 - 750 Hz; accelerometer CA300.

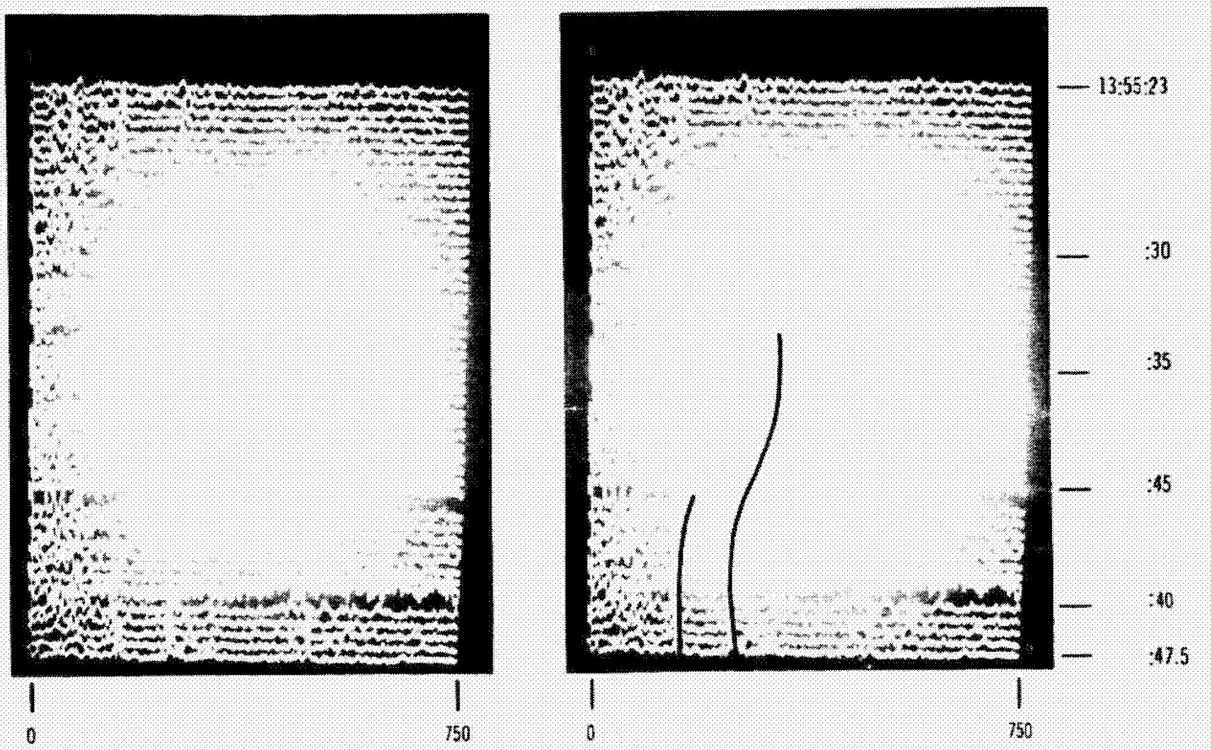

Figure 18. - Acceleration power spectral density versus frequency at $\frac{1}{2}$ second intervals for Titan Centaur 1 flight. 0 - 750 Hz; accelerometer CA300.

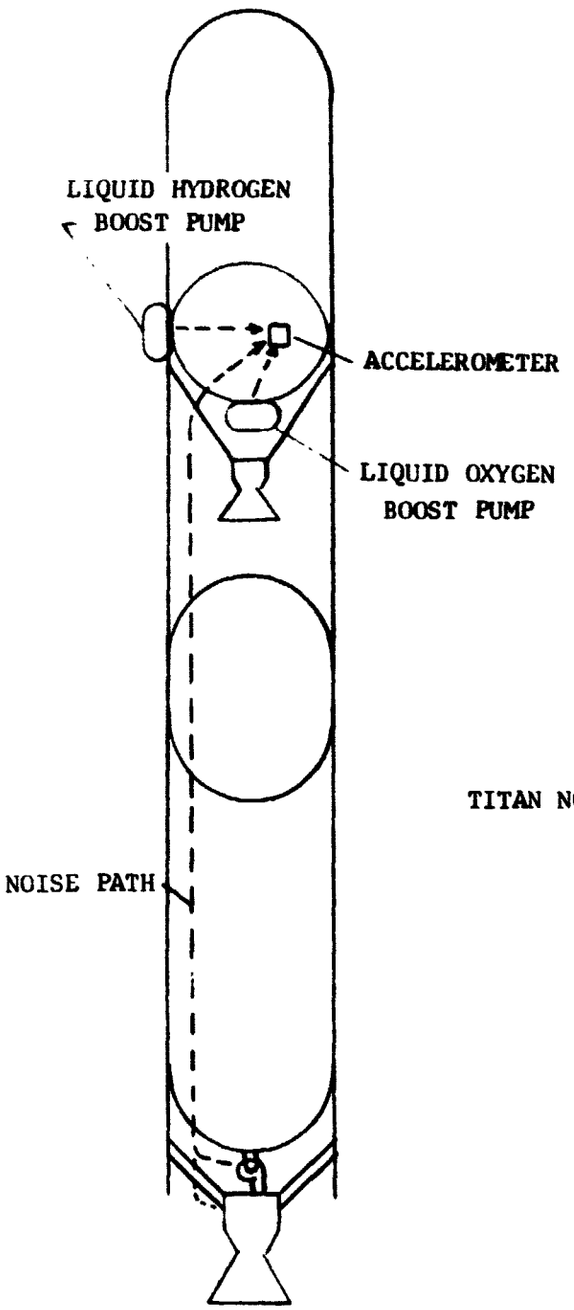

FIGURE 19a. PHYSICAL SYSTEM SCHEMATIC

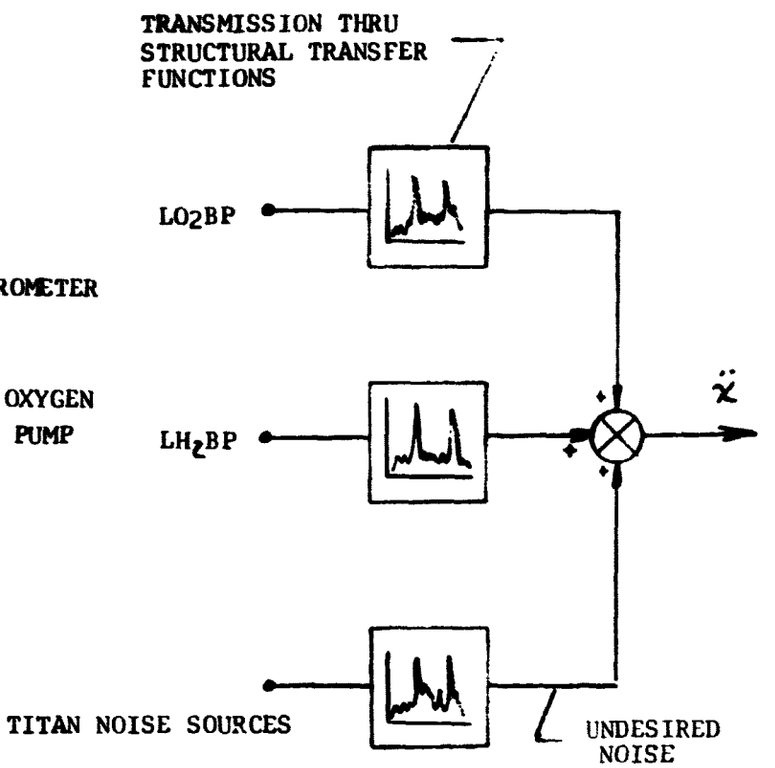

FIGURE 19b. BLOCK DIAGRAM

FIGURE 19. THE ENHANCEMENT PROBLEM